

Thieno[3,4-*b*]thiophene-Based Organic Dyes for Dye-Sensitized Solar Cells

Yung-Chung Chen,^[a] Hsien-Hsin Chou,^[a] Ming Chih Tsai,^[a, b] Sheng-Yu Chen,^[a]
Jiann T. Lin,^{*[a]} Ching-Fa Yao,^{*[b]} and Kellen Chen^[c]

Abstract: New dipolar sensitizers containing an ethyl thieno[3,4-*b*]thiophene-2-carboxylate (ETTC) entity in the conjugated spacer have been synthesized in two isomeric forms. These compounds were used as the sensitizers of n-type dye-sensitized solar cells (DSSCs). The best conversion efficiency (5.31 %) reaches approximately 70 % of the N719-based (7.41 %) DSSC

fabricated and measured under similar conditions. The ETTC-containing compounds exhibit a bathochromic shift of the absorption compared to their thio-

Keywords: dye-sensitized solar cells • electron transfer • metal-free sensitizers • quantum chemistry • quinoids

phene congeners due to the quinoid effect, however, charge-trapping at the ester group of ETTC was found to jeopardize the electron injection and lower the cell efficiency. Charge trapping is alleviated as the ester group of ETTC is replaced with a hydrogen atom, as evidenced from the theoretical computation.

Introduction

To keep pace with ever increasing demand of energy supply accompanying global economy's growth, search for alternative energy sources has become one of the most important issues for governments and scientists. Though nuclear power plant plays an important role in mankind civilization, the recent disaster in Japan arouses some doubts on its long-term reliability. Among different choices of new energy sources, solar energy is considered to be very attractive because of its sustainability and abundant supply. In spite of good solar-to-electricity conversion efficiency, the high price prohibits large scale application of silicon-based solar cells. Therefore, more and more researchers turn their interests to organic photovoltaic cells (OPVs)^[1] and dye-sensitized solar cells (DSSCs).^[2] Considerable progress has been made on dye-sensitized solar cells for the past two decades since the seminal report by O'Reagan and Grätzel in 1991.^[3] Efficiencies surpassing 11 % have been achieved by ruthenium dyes^[4] and Zn-porphyrin dye-based^[5] DSSCs. Compared with

these two classes of dyes, metal-free dyes normally absorb at shorter wavelength, which results in a lower cell efficiency. Nonetheless, a promising cell efficiency of > 10 % was reported recently by Wang and co-workers.^[6]

Electron-transfer dynamics strongly affects the performance of DSSCs,^[7] and this dynamics certainly correlates with the molecular structure of the sensitizer.^[8] Therefore, even though light harvesting of sensitizers is of paramount importance, exploration of sensitizers for better correlation of structure with cell performance should not be overlooked. With this in mind, we set out to search for possible candidates which have similar structures for fair comparison. In recent years, we have developed some series of amine-based metal-free dipolar sensitizers for n-type DSSCs in which the sensitizers were adsorbed on the nanocrystalline TiO₂, a n-type semiconductor.^[9] In one case where thiazole entity was used in the conjugated spacer, we found that the sensitizer with heteroatoms on the thiazole ring away from the acceptor exhibited much better cell performance than its isomer having heteroatoms closer to the acceptor.^[9] Therefore, the ethyl thieno[3,4-*b*]thiophene-2-carboxylate (ETTC) entity was chosen for our purpose based on the following reasons: 1) ETTC and congeners have been widely used for construction of low-band gap polymers for OPV applications because of their favorable quinoid structure;^[1c,10] this characteristic may help to redshift the absorption spectra. 2) ETTC can be inserted in the conjugated spacer where the sulfur atom of the thiophene-2-carboxylate is either closer to or away from the acceptor. Therefore, the two possible isomeric structures allow systematic studies for comparison. In this paper we will report the syntheses of two series of isomeric sensitizers based on ETTC and their applications in n-type DSSCs. In addition, quantum chemistry computation was carried out to elucidate the different behaviors of the two isomers.

[a] Y.-C. Chen, H.-H. Chou, M. C. Tsai, S.-Y. Chen, J. T. Lin
Institute of Chemistry, Academia Sinica
11529, Nankang, Taipei (Taiwan)
Fax: (+886) 783-1237
E-mail: jtlin@chem.sinica.edu.tw

[b] M. C. Tsai, C.-F. Yao
Department of Chemistry
National Taiwan Normal University
117, Taipei (Taiwan)
E-mail: cheyao@ntnu.edu.tw

[c] K. Chen
AU Optronics Corporation
30078, Hsinchu (Taiwan)

Supporting information for this article is available on the WWW under <http://dx.doi.org/10.1002/chem.201200012>.

Results and Discussion

Synthesis of the materials: The structures of new dyes are illustrated in Figure 1. The compounds are classified into two types of isomers, **MCT-*n*** and **FTT-*n*** (*n*=1–5). The syntheti-

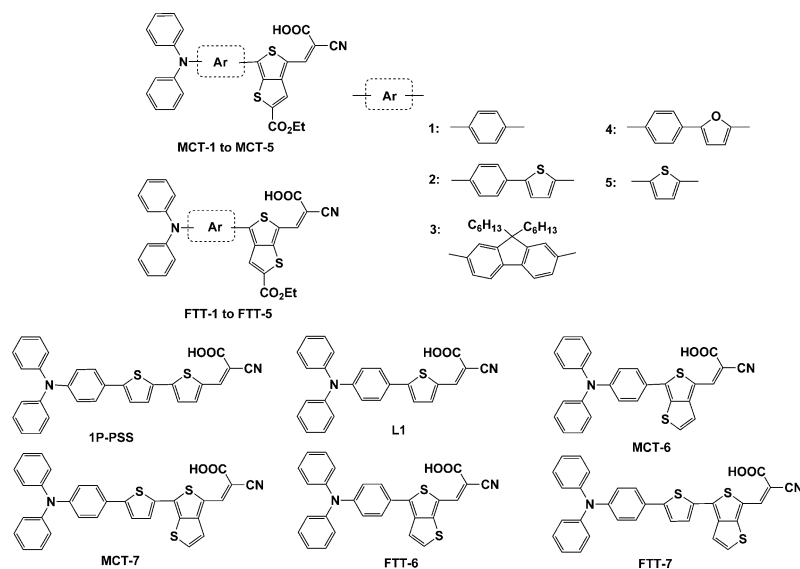


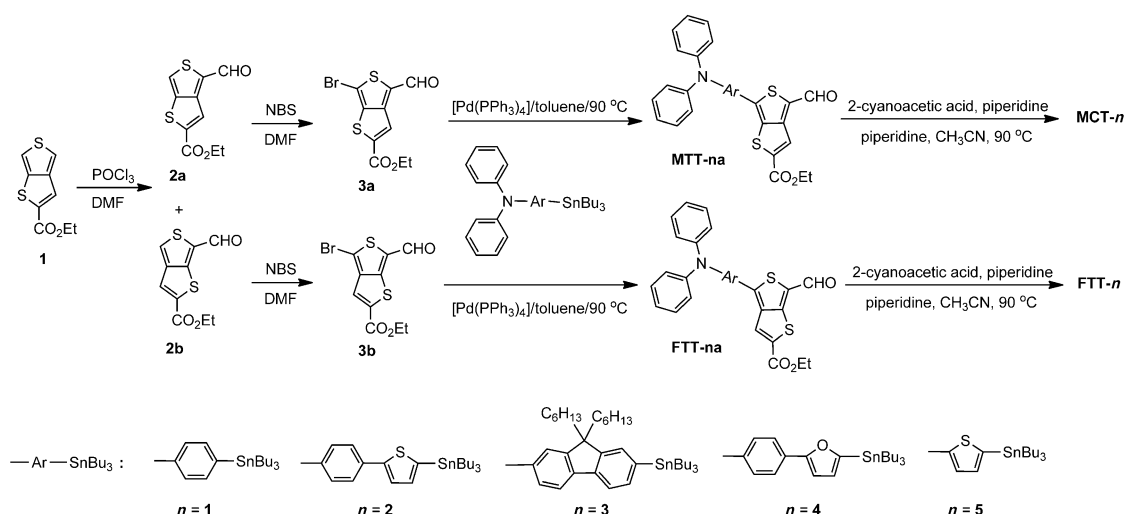
Figure 1. Structures of **MCT**, **FTT** dyes and referenced dyes (**1P-PSS** and **L1**).

cal protocol of the compounds is illustrated in Scheme 1. Thieno[3,4-*b*]thiophene-2-carboxylic acid ethyl ester (**1**) was prepared according to the published procedures.^[11] Formylation of **1** via Vilsmeier–Haack reaction led to two isomers, **2a** (35%) and **2b** (18%). Compound **3a** (or **3b**) was obtained from **2a** (or **2b**) via bromination with NBS. The two compounds then underwent palladium catalyzed Stille coupling^[12] reaction with appropriate stannyl reagents to provide formyl compounds **MCT-*n*** (or **FTT-*n***). Finally, the

Knoevenagel condensation of **MCT-*n*** (or **FTT-*n***) with cyanoacetic acid afforded the desired products.

Optical properties: The optical absorption spectra of the dyes in THF are displayed in Figure 2 and the data are collected in Table 1. The long wavelength absorption at >470 nm is from more delocalized π – π^* transition with charge-transfer character, and the bands at <400 nm are due to localized π – π^* transition. The λ_{max} (or E_{0-0} from the intersection of the absorption and emission spectra) value of the charge transfer band for the two series of compounds decreases in the order of **MCT-5** > **MCT-2** > **MCT-4** > **MCT-1** > **MCT-3** and **FTT-5** > **FTT-2** > **FTT-4** > **FTT-1** > **FTT-3**, respectively. Replacement of a phenyl unit by a thienyl unit (**5** vs. **1**) results in considerable red shift of the λ_{max} value, which is consistent with the trend normally observed in nonlinear optical chromo-

phores^[13] and is attributed to a lower delocalization energy of thiophene than benzene.^[14] Similarly, **2** and **4** have a larger λ_{max} value than **3** despite of planarity of the fluorene entity. Though furan has smaller resonance energy compared to thiophene, compounds with a thiophene entity in the spacer have a shorter λ_{max} value than their furan congeners, that is, **2** versus **4**. This phenomenon is in conformity with the trend observed in nonlinear optical chromophores.^[13b,d] Dye **3** absorbs at shorter wavelength than **1**, indicat-



Scheme 1. Synthesis of the dyes.

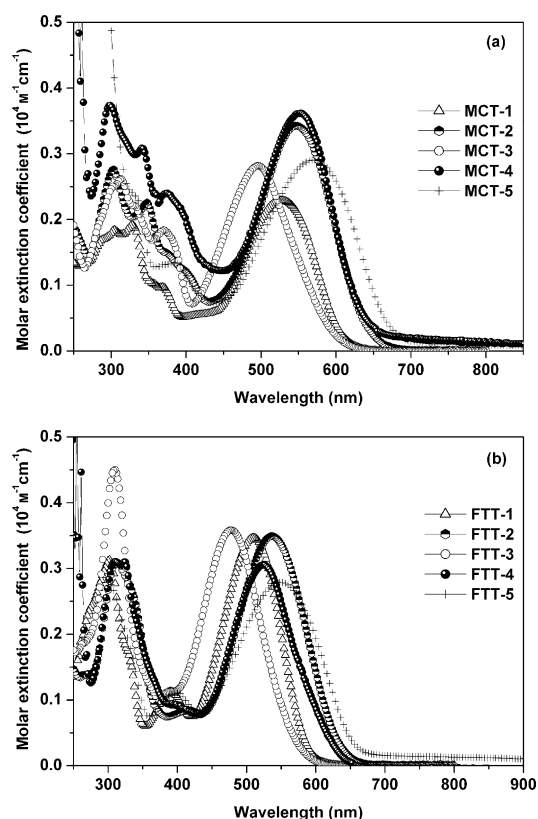


Figure 2. Absorption spectra of a) **MCT** and b) **FTT** dyes in THF solutions.

ing that an extra phenylene in **3** jeopardizes the electronic communication between the donor and the acceptor.

It is very interesting that the ETTC entity is better than the thiophene entity in redshifting the absorption band. For example, the λ_{max} values of **MCT-1** (or **FTT-1**) and **MCT-2** (or **FTT-2**) are larger than those of **1P-PSS**^[15] ($\lambda_{\text{max}} = 461 \text{ nm}$, $\epsilon = 27100 \text{ M}^{-1} \text{ cm}^{-1}$) and **L1**^[16] ($\lambda_{\text{max}} = 444 \text{ nm}$, $\epsilon = 27490 \text{ M}^{-1} \text{ cm}^{-1}$), respectively. Likely, both quinoid structure of ETTC and the electron-withdrawing ester moiety play

Table 1. Electrooptical parameters of the dyes.

Dye	λ_{abs} ($\epsilon \times 10^{-4} \text{ M}^{-1} \text{ cm}^{-1}$) [nm] ^[a]	λ_{em} [nm] ^[a]	E_{ox} [mV] ^[b]	HOMO/LUMO [eV]	E_{0-0} [eV] ^[c]	E_{0-0}^* [V] ^[d]
MCT-1	328 (1.92), 524 (2.29)	644	545 (119)	5.35/3.30	2.05	-0.70
MCT-2	302 (2.76), 546 (3.42)	661	444 (124), 681 (153)	5.24/3.31	1.93	-0.69
MCT-3	313 (2.62), 496 (2.81)	612	549 (196)	5.35/3.26	2.09	-0.74
MCT-4	302 (2.78), 553 (3.62)	624	446 (100), 680 (na)	5.25/3.29	1.96	-0.71
MCT-5	329 (2.39), 382 (1.37), 570 (2.92)	694	434 (113)	5.23/3.41	1.82	-0.59
FTT-1	302 (3.13), 509 (3.47)	629	613 (121)	5.41/3.29	2.12	-0.71
FTT-2	312 (3.10), 536 (3.49)	623	448 (110), 684 (113)	5.25/3.29	1.96	-0.71
FTT-3	310 (4.40), 477 (3.58)	593	523 (86)	5.32/3.14	2.18	-0.86
FTT-4	310 (3.11), 523 (3.05)	618	452 (90), 704 (na)	5.25/3.25	2.00	-0.75
FTT-5	398 (1.12), 548 (2.80)	664	380 (109)	5.18/3.30	1.88	-0.70

[a] Recorded in THF solutions at 298 K. [b] Recorded in THF solutions. $E_{\text{ox}} = 1/2(E_{\text{pa}} + E_{\text{pc}})$, $\Delta E_{\text{p}} = E_{\text{pa}} - E_{\text{pc}}$ where E_{pa} and E_{pc} are peak anodic and cathodic potentials, respectively. Oxidation potential reported is adjusted to the potential of ferrocene which was used as an internal reference. The values in parentheses are the peak separation of cathodic and anodic waves. Scan rate: 100 mV s^{-1} . [c] The bandgap, E_{0-0} , was derived from the intersection of the absorption and emission spectra. [d] E_{0-0}^* : The excited state oxidation potential versus NHE.

important roles in this behavior (see below). Another interesting feature is that the charge transfer band of **MCT** compounds has longer λ_{max} and smaller molar extinction coefficient than that of **FTT** congeners. This may be attributed to the better charge trapping effect of the ester moiety in **MCT** compounds (see below), which significantly lowers the LUMO energy level and reduce the transition probability from the ground state to the first excited state. Emission spectra of the compounds follow the same trend as the absorption spectra except for the order of **1** and **4**. The longer emission wavelength of **1** than **4** suggests that there is more geometrical relaxation for the lowest emissive excited state of the former.

Electrochemical properties: The electrochemical properties of the dyes were investigated by using cyclic voltammetry (CV) method, and relevant data are presented in Table 1. Selected cyclic voltammograms are shown in Figure 3. A

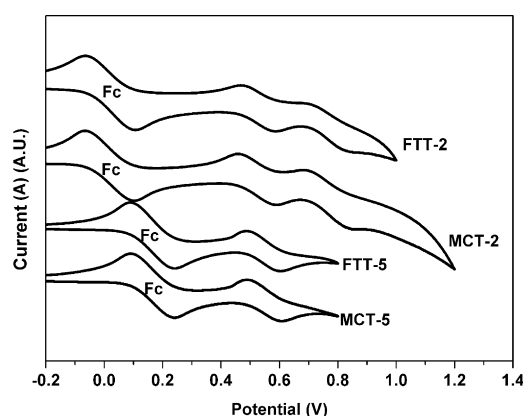


Figure 3. Cyclic voltammograms of the dyes recorded in CH_2Cl_2 (scan rate 100 mV s^{-1}).

quasi-reversible one-electron oxidation wave detected at about 380–613 mV more positive than ferrocene/ferrocenium is attributed to the removal of electron from the arylamine. Similar to our previous observations, direct attachment of electron excessive thiophene at the nitrogen atom of arylamine significantly lowers the oxidation potential of the arylamine.^[17] As expected, compounds **MCT-5** and **FTT-5** have the lowest oxidation potentials among all. Compounds without electron excessive thiophene or furan ring in the spacer, **MCT-1**, **MCT-3**, **FTT-1**, and **FTT-3**, are oxidized at higher potentials. A second quasi-reversible one-electron oxidation wave at a higher potential was discernible for **MCT-2**, **MCT-4**, **FTT-2**, and **FTT-4**, indicating the presence of thiophene or furan

helped to stabilize the dications formed. There is no obvious trend in the first oxidation potential between the isomeric pair of **MCT** and **FTT**.

Photocurrent–voltage characteristics: The dye-sensitized solar cells were fabricated by using these dyes as the sensitizers for nanocrystalline anatase TiO₂. Typical solar cells, with an effective area of 0.25 cm², were fabricated with an electrolyte composed of 0.05 M I₂/0.5 M LiI/0.5 M 4-*tert*-butylpyridine in acetonitrile solution. The device performance statistics under AM 1.5 illumination are collected in Table 2. Figure 4 and Figure 5 show the photocurrent–voltage (*J*–*V*) curves and the incident photon-to-current conversion effi-

Table 2. DSSCs performance parameters of the dyes.

Sample	<i>V</i> _{OC} [V]	<i>J</i> _{SC} [mA cm ⁻²]	FF	η [%]	Dye loading [10 ⁻⁷ mol cm ⁻²]
MCT-1	0.56	8.80	0.69	3.40	2.73
MCT-2	0.52	4.86	0.69	1.72	3.68
MCT-3	0.58	8.14	0.70	3.30	5.29
MCT-4	0.50	3.64	0.68	1.23	4.63
MCT-5	0.44	2.92	0.52	0.66	3.09
FTT-1	0.61	12.6	0.66	5.03	3.72
FTT-2	0.54	9.21	0.66	3.26	4.14
FTT-3	0.64	12.2	0.68	5.31	1.78
FTT-4	0.53	7.52	0.66	2.65	3.12
FTT-5	0.51	6.64	0.65	2.17	2.57
N719	0.72	16.1	0.64	7.41	1.46

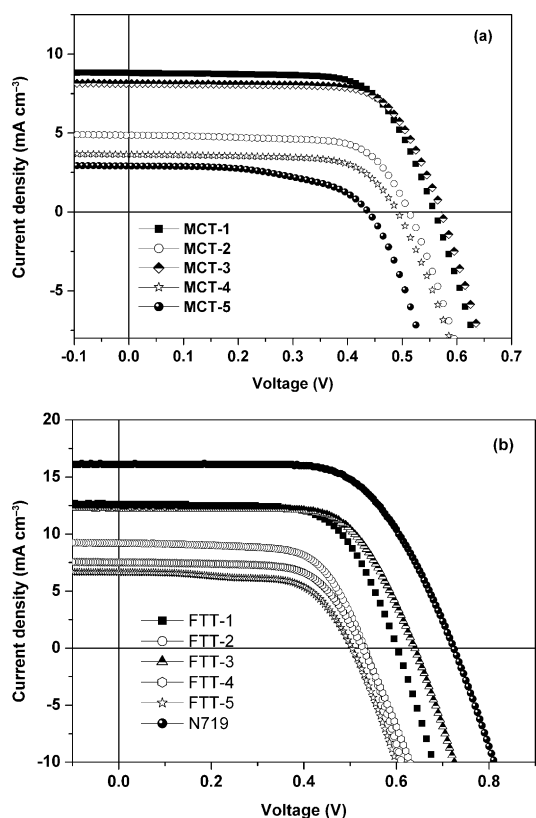


Figure 4. Current density/voltage curves of DSSCs based on the a) **MCT** and b) **FTT** dyes under AM 1.5 solar simulator of 100 mW cm⁻². Cell area = 0.25 cm².

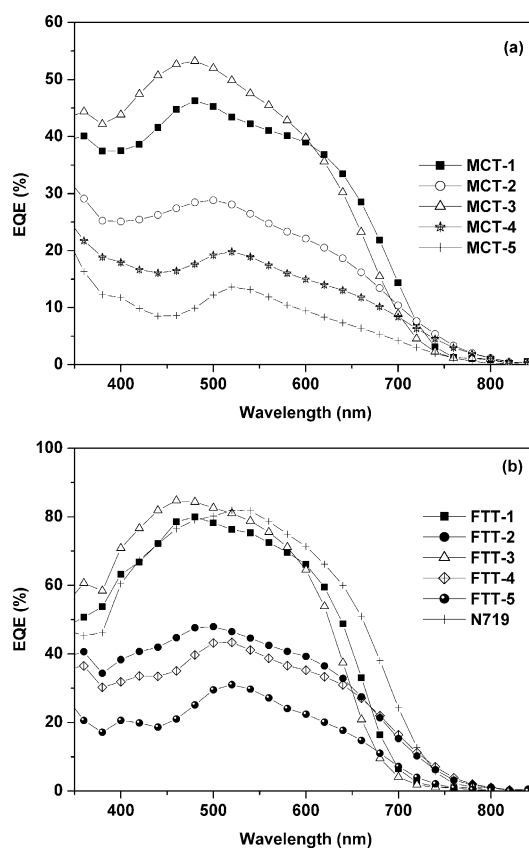


Figure 5. IPCE plots for the DSSCs using a) **MCT** and b) **FTT** dyes.

ciencies (IPCE) of the cells. The conversion efficiencies appear to be lower than that of N719-based cell (N719 = bis(tetrabutylammonium)-*cis*-di(thiocyanato)-*N,N'*-bis(4-carboxylato-4'-carboxylic acid-2,2'-bipyridine)ruthenium) fabricated and measured under similar conditions. **FTT** compounds exhibited better cell efficiencies than **MCT** congeners. DSSCs based on **FTT-1** and **FTT-3** have the best performance among all, with efficiencies reaching about 70% of the standard cell.

To elucidate the factors affecting the performance of the cells, the adsorbed dye densities of the sensitizers on TiO₂ surface were measured (Table 2). Obviously dye density alone is not the decisive factor for the cell performance. For example, the dye density of **MCT-3** is nearly three times compared with **FTT-3**. However, the conversion efficiency of DSSC based on **MCT-3** is only 62% of the cell based on **FTT-3**. Both open-circuit voltage (*V*_{OC}) and short-circuit current (*J*_{SC}) of **FTT** compounds are higher than those of **MCT** series. The higher *J*_{SC} values of the **FTT**-based DSSCs are most likely stemmed from more efficient electron injection from the dye to the TiO₂ surface (see below), besides partial contribution from larger molar extinction coefficients of **FTT** than **MCT**. Effective suppression of dark current normally leads to a higher *V*_{OC}. The dark currents of DSSCs fabricated were also checked (Figure 6). The cells of **1** and **3** in both series have lower dark currents and therefore higher *V*_{OC} values. In comparison, cells of **5** have the highest dark

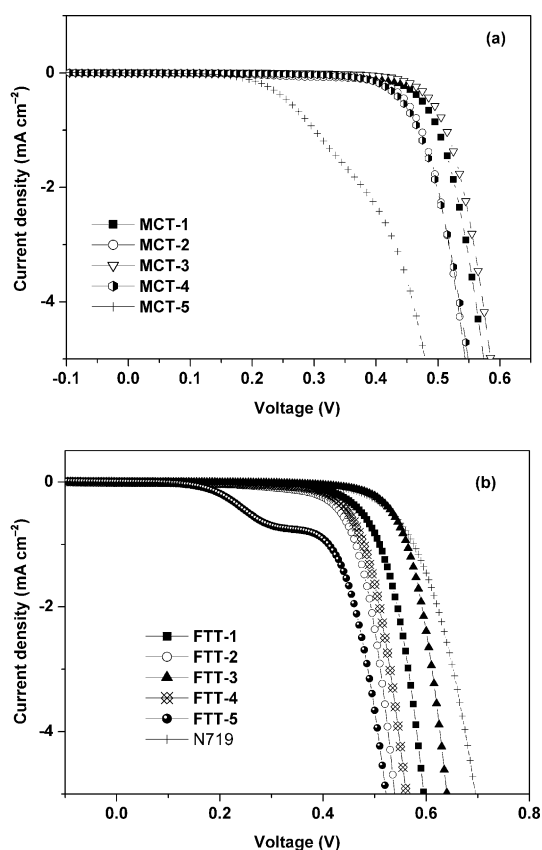


Figure 6. Dark current of DSSCs based on a) **MCT** and b) **FTT** dyes.

currents and the lowest V_{OC} among all. Somewhat higher V_{OC} found in the **FTT**-based DSSCs cannot be rationalized by the dark current. We speculate the **FTT** dyes adsorbed on TiO_2 nanoparticles raised the Fermi level compared the **MCT** dyes. The aforementioned arguments on dark current were supported by the electrochemical impedance spectroscopic (EIS) studies carried out in the dark. The intermediate frequency semicircle in the electrochemical impedance spectra (Figure S1 in the Supporting Information) represents the charge transfer phenomena between the TiO_2 surface and the electrolyte, that is, dark current. Efficient suppression of the dark current leads to larger semicircle. The resistance towards the dark current (the size of semicircle) decreases in the order of **MCT-3** > **MCT-1** > **MCT-2** > **MCT-4** > **MCT-5** and **FTT-3** > **FTT-1** > **FTT-2** > **FTT-4** > **FTT-5**, respectively.

Electrochemical impedance upon illumination of 100 mW cm^{-2} was also measured under open-circuit condition, and the Nyquist plots of DSSCs with different dyes are shown in Figure S2 in the Supporting Information. The radius of the intermediate frequency semicircle (10^{-2} – 10^5 Hz) in the Nyquist plot will reflect electron-transport resistance, and the smaller radius means the lower electron transport resistance. Though overlapping of the first and the second semicircles prevented us from unambiguous calculation of the electron transport resistance in most cases, the order of the electron transport resistance could be estimat-

ed. The electron transport resistance of **5**, **4**, and **2** in both series of compounds is significantly larger than that of **3** and **1**, and decreases in the order of **MCT-5** >> **MCT-4** > **MCT-2** and **FTT-5** >> **FTT-4** > **FTT-2**, respectively. This is consistent with the better cell performance of **1**- and **3**-based DSSCs. Moreover, **MCT**-based cells have larger resistance than **FTT**-based cells, which is in conformity with their lower efficiencies.

Theoretical approach: Quantum chemistry computation was conducted for the compounds in order to gain further insight for the correlation between the structure and the physical property as well as the cell performance, and the results for the theoretical approach are included in Table S1 in the Supporting Information. Computations on compounds **MCT-6** (or **FTT-6**), and **MCT-7** (or **FTT-7**), in which the ester group in **MCT-1** (or **FTT-1**) and **MCT-2** (or **FTT-2**) was replaced by a hydrogen atom (Figure 1), were also carried out for comparison. The computed frontier orbitals of the compounds and their corresponding energy states are included in Figure S3 and Figure S4 in the Supporting Information, respectively. In the optimized structure, no significant deviation from planarity was found in the spacer between the ETTC and 2-cyanoacrylic acid or heteroaromatic ring (Figure 7). The dihedral angles between ETTC and phenyl or fluorenyl ring (ca. 31 to 35°) are larger than those between ETTC and thienyl or furyl ring (ca. 10 to 20°). The larger dihedral angle will jeopardize the charge transfer and result in blue shift of the absorption band: **MCT-1**, **MCT-3**, **FTT-1** and **FTT-3** have smaller λ_{max} values among the series of compounds (see above). The HOMO orbitals in these compounds are mainly composed of the diarylamine with contributions from the neighboring spacer extending to ETTC entity and the 2-cyanoacrylic acid. In comparison, the LUMO orbitals are mainly composed of 2-cyanoacrylic acid moiety and ETTC extending to the spacer. The charge transfer character of the $S_0 \rightarrow S_1$ transition is therefore evident. Figure 8 shows HOMO and LUMO orbitals of four representative compounds, **MCT-2**, **FTT-2**, **MCT-6** and **FTT-6** (see below).

The Mulliken charges shifts for the S_1 and S_2 states were also calculated from the TDDFT results. Differences in the Mulliken charges in the excited and ground states were calculated and grouped into several segments (Figure S5 in the Supporting Information), diphenylamino (Am), aromatic ring (Ph, Flu6, T, or F), ETTC (Tt'c2 or Tt'c2) and 2-cyanoacrylic acid (Ac), to estimate the extent of charge separation upon excitation (Table S1 in the Supporting Information). Figure S5 displays the changes in Mulliken charges of all dyes for the $S_0 \rightarrow S_1$ and $S_0 \rightarrow S_2$ transitions. There is significant charge transfer from the arylamine donor to the 2-cyanoacrylic acid acceptor for $S_0 \rightarrow S_1$ transition, and the negative charge accumulated at 2-cyanoacrylic acid (Ac) ranges from -0.19 to -0.31 . There is even higher negative charge accumulated at the ETTC entity (-0.34 to -0.53). Compared to **FTT** compounds, **MCT** compounds were found to have more negative charge accumulated at the ETTC unit.

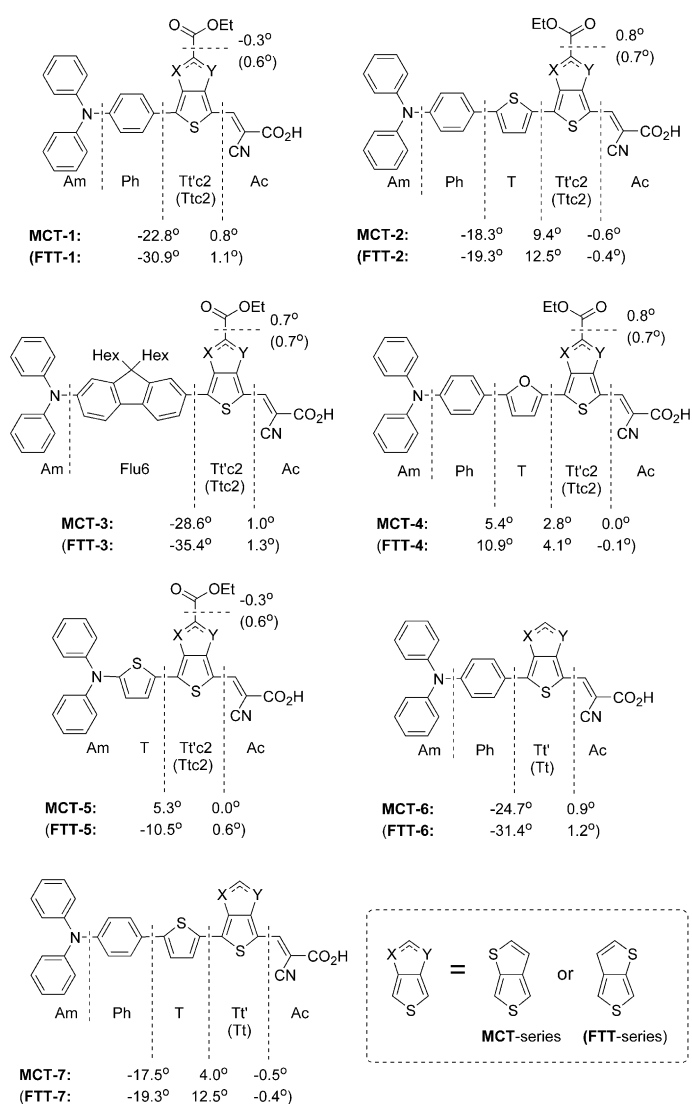
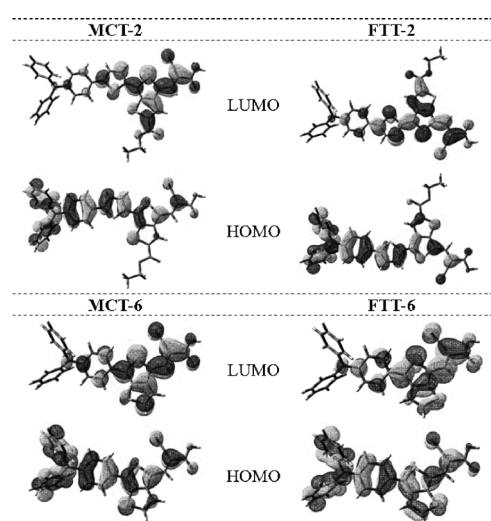


Figure 7. Schematic division and dihedral angles of molecules.

Figure 8. HOMO and LUMO orbitals of dyes **MCT-2**, **FTT-2**, **MCT-6**, and **FTT-6**.

Moreover, the ester of ETTC in **MCT** has higher negative charge than that in **FTT**. Though the extra thiophene ring of ETTC will lead to better stabilization during formation of the quinoid structure, the charge trapping effect of the ester moiety may lower the cell efficiencies of **MCT**-based DSSCs due to less efficient electron injection. Similar behavior was found in sensitizers incorporating a cyanovinyl entity in the spacer.^[9f] Computations on compounds **MCT-6** (or **FTT-6**), and **MCT-7** (or **FTT-7**) offer us an opportunity for closer inspection of the role of the ester group in these compounds. Note that Ttc2 or Tt'c2 used for **FTT** and **MCT** compounds have now been changed to Tt and Tt', respectively. The $f \times \Delta q$ value (the product of the oscillator strength and the Mulliken charge changes in the terminal Ac group) of the Ac entity for the $S_0 \rightarrow S_1$ transition, an approximate measure for the electronic coupling strength from the dye molecule to the attached TiO_2 nanoparticle, increases in both **FTT** and **MCT** dyes: **FTT-1**: -0.18, **FTT-6**: -0.21; **MCT-1**: -0.13, **MCT-6**: -0.21; **FTT-2**: -0.18, **FTT-7**: -0.25; **MCT-2**: -0.18, **MCT-7**: -0.24. Therefore, we anticipate that there is more facile electron injection and the efficiencies of DSSCs can be further improved as the ester group of ETTC is replaced by a hydrogen atom or an alkyl group. It is also interesting to note that **MCT** and **FTT** compounds have comparable absorption wavelength and the oscillator strength as the ester group of ETTC is replaced by a hydrogen atom, indicating the impact of the ester group on the electronic properties of the molecules.

Conclusion

In summary, we have synthesized two series of isomeric sensitizers containing a ethyl thieno[3,4-*b*]thiophene-2-carboxylate (ETTC) entity in the conjugated spacer, **MCT** (with the sulfur atom of the thiophene-2-carboxylate in ETTC lying away from the acceptor) and **FTT** (with the sulfur atom of the thiophene-2-carboxylate in ETTC lying closer to the acceptor). We also explored their applications in n-type DSSCs. The best conversion efficiency reaches 5.31%, which is 71% of the N719-based DSSC fabricated and measured under similar conditions. The **MCT** isomer has longer wavelength absorption with weaker absorption intensity than the **FTT** isomer. Both **MCT** and **FTT** compounds exhibit bathochromic shift of the charge transfer absorption compared to their thiophene congeners due to energetically favorable quinoid structure of ETTC than thiophene. However, charge-trapping of the ester moiety at the ETTC entity hampers efficient electron injection, and there is more serious charge trapping in **MCT** dyes. As the ester group of ETTC is replaced with a hydrogen atom, the charge trapping can be alleviated and better charge injection is expected.

Experimental Section

General information: Unless otherwise specified, all the reactions were performed under nitrogen atmosphere using standard Schlenk techniques. All solvents used were purified by standard procedures, or purged with nitrogen before use. All chromatographic separations were carried out on silica gel (60M, 230–400 mesh). ¹H NMR and ¹³C NMR spectra were recorded on a Bruker 400 MHz spectrometer. Mass spectra (FAB) were recorded on a VG70–250S mass spectrometer. Elementary analyses were performed on a Perkin–Elmer 2400 CHN analyzer. Absorption spectra were recorded on a Cary 50 probe UV/Vis spectrophotometer. Fluorescence spectra were recorded on a Hitachi F-4500 Spectrophotometer. Cyclic voltammetry experiments were performed with a CHI-621B electrochemical analyzer. All measurements were carried out at room temperature with a conventional three electrode configuration consisting of a platinum working electrode, an auxiliary electrodes and a non-aqueous Ag/AgNO₃ reference electrode. The photoelectrochemical characterizations on the solar cells were carried out using an Oriel Class A solar simulator (Oriel 91195 A, Newport Corp.). Photocurrent–voltage characteristics of the DSSCs were recorded with a potentiostat/galvanostat (CHI650B, CH Instruments, Inc.) at a light intensity of 100 mWcm⁻² calibrated by an Oriel reference solar cell (Oriel 91150, Newport Corp.). The monochromatic quantum efficiency was recorded through a monochromator (Oriel 74100, Newport Corp.) at short circuit condition. The intensity of each wavelength was in the range of 1 to 3 mWcm⁻². Electrochemical impedance spectra (EIS) were recorded for DSSC under illumination at open-circuit voltage (*V*_{OC}) or dark at –0.42 V potential at room temperature. The frequencies explored ranged from 10 mHz to 100 kHz. The TiO₂ nanoparticles and **N719** were purchased from Solaronix S. A., Switzerland.

Synthesis of ethyl 4-(4-(diphenylamino)phenyl)-6-formylthieno[3,4-b]thiophene-2-carboxylate (FTT-1a): In a two-necked flask was loaded a mixture of ethyl-4-bromo-6-formylthieno[3,4-b]thiophene-2-carboxylate (**3b**, 0.14 g, 0.44 mmol), *N,N*-diphenyl-4-(4,4,5,5-tetramethyl-1,3,2-dioxaborolan-2-yl)aniline (0.20 g, 0.53 mmol), Pd(PPh₃)₄ (30 mg), 2 M Na₂CO_{3(aq)} (2 mL), ethanol (2 mL) and toluene (40 mL) under nitrogen atmosphere and refluxed overnight. After cooling, the reaction was quenched with aqueous NH₄Cl and extracted with CH₂Cl₂. The organic extracts were washed with brine solution and dried over anhydrous MgSO₄. After filtration, the filtrate was pumped dry and the crude product was purified by column chromatography using CH₂Cl₂/hexane (1:1 by vol) and EA/hexane (1:9 by vol) as the eluent successively to provide **FTT-1a** in 89% yield. ¹H NMR (400 MHz, CDCl₃): δ = 9.85 (s, 1H), 7.99 (s, 1H), 7.58 (d, *J* = 8.8 Hz, 2H), 7.32 (t, *J* = 7.6 Hz, 4H), 7.17–7.09 (m, 8H), 4.38 (q, *J* = 7.6 Hz, 2H), 1.39 ppm (t, *J* = 7.2 Hz, 3H).

Synthesis of (E)-2-cyano-3-(4-(4-(diphenylamino)phenyl)-2-(ethoxycarbonyl)thieno[3,4-b]thiophen-6-yl)acrylic acid (FTT-1): A mixture of **FTT-1a** (0.19 g, 0.39 mmol), cyanoacetic acid (65 mg, 0.78 mmol), acetonitrile (20 mL), and piperidine (5 drops) was placed into a 300 mL flask and refluxed for overnight. After cooling, the organic precipitate was collected by filtration, and washed with ether and water. The crude product was purified by column chromatography using EtOH/CH₂Cl₂ (1:9 by vol) as the eluent. The product was further recrystallized with ether/hexane to provide **FTT-1** in 60% yield. ¹H NMR (400 MHz, [D₈]THF): δ = 8.48 (s, 1H), 8.20 (s, 1H), 7.90 (d, *J* = 8.4 Hz, 2H), 7.50 (t, *J* = 7.6 Hz, 4H), 7.35 (d, *J* = 7.6 Hz, 4H), 7.13 (t, *J* = 7.6 Hz, 2H), 7.07 (d, *J* = 8.4 Hz, 2H), 4.40 (q, *J* = 7.2 Hz, 2H), 1.39 ppm (t, *J* = 7.2 Hz, 3H); ¹³C NMR (125 MHz, [D₈]THF): δ = 164.2, 162.5, 152.8, 151.0, 147.8, 147.4, 142.6, 141.1, 140.5, 130.6, 129.9, 126.7, 126.0, 125.4, 124.6, 122.7, 120.7, 117.0, 97.8, 62.7, 14.7 ppm; MS (FAB): *m/z* 551.1 (*M*⁺); elemental analysis calcd (%) for C₃₁H₂₂N₂O₄S₂: C 67.62, H 4.03, N 5.09; found: C 67.78, H 4.01, N 4.95.

Other compounds are described in detail in the Supporting Information.

Assembly and characterization of DSSCs: The photoanode used was the TiO₂ thin film (12 μm of 20 nm particles as the absorbing layer and 6 μm of 400 nm particles as the scattering layer) coated on FTO glass substrate^[18] with a dimension of 0.5 × 0.5 cm², and the film thickness measured by a profilometer (Dektak3, Veeco/Sloan Instruments Inc., USA).

A platinumized FTO produced by thermopyrolysis of H₂PtCl₆ was used as a counter electrode. The TiO₂ thin film was dipped into the THF solution containing 3 × 10⁻⁴ M dye sensitizers for at least 12 h. After rinsing with THF, the photoanode adhered with a polyester tape of 30 μm in thickness and with a square aperture of 0.36 cm² was placed on top of the counter electrode and tightly clipping them together to form a cell. Electrolyte was then injected into the space and then sealing the cell with the Torr Seal[®] cement (Varian, MA, USA). The electrolyte was composed of 0.5 M lithium iodide (LiI), 0.05 M iodine (I₂), and 0.5 M 4-*tert*-butylpyridine that was dissolved in acetonitrile.

Quantum chemistry calculations: The computation were performed with Q-Chem 4.0 software.^[19] Geometry optimization of the molecules were performed using hybrid B3LYP functional and 6–31G* basis set. For each molecule, a number of possible conformations were examined and the one with the lowest energy was used. The same functional was also applied for the calculation of excited states using time-dependent density functional theory (TD-DFT). There exist a number of previous works that employed TD-DFT to characterize excited states with charge-transfer character.^[20] In some cases underestimation of the excitation energies was seen.^[21] Therefore, in the present work, we use TD-DFT to visualize the extent of transition moments as well as their charge-transfer characters, and avoid drawing conclusions from the excitation energy.

Acknowledgements

We acknowledge the support of the Academia Sinica (AC) and NSC (Taiwan), AUO Optronics Corp. and the Instrumental Center of Institute of Chemistry (AC).

- [1] a) C. J. Brabec, S. Gowrisanker, J. J. M. Halls, D. Laird, S. Jia, S. P. Williams, *Adv. Mater.* **2010**, *22*, 3839; b) W. Cai, X. Gong, Y. Cao, *Sol. Energy Mater. Sol. Cells* **2010**, *94*, 114; c) D. Gendron, M. Leele, *Energy Environ. Sci.* **2011**, *4*, 1225.
- [2] a) J. Preat, D. Jacquemin, E. A. Perpète, *Energy Environ. Sci.* **2010**, *3*, 891; b) Z. Ning, Y. Fu, H. Tian, *Energy Environ. Sci.* **2010**, *3*, 1170.
- [3] B. O'Reagen, M. Grätzel, *Nature* **1991**, *353*, 737.
- [4] a) F. Gao, Y. Wang, D. Shi, J. Zhang, M. Wang, X. Jing, R. Humphry-Baker, P. Wang, S. M. Zakeeruddin, M. Grätzel, *J. Am. Chem. Soc.* **2008**, *130*, 10720; b) C.-Y. Chen, M. Wang, J.-Y. Li, N. Pootrakulchote, L. Alababai, C.-H. Ngocle, J.-D. Decoppet, J.-H. Tsai, C. Grätzel, C.-G. Wu, S. M. Zakeeruddin, M. Grätzel, *ACS Nano* **2009**, *3*, 3103.
- [5] a) T. Bessho, S. M. Zakeeruddin, C.-Y. Yeh, E. W.-G. Diau, M. Grätzel, *Angew. Chem.* **2010**, *122*, 6796; *Angew. Chem. Int. Ed.* **2010**, *49*, 6646; b) A. Yella, H.-W. Lee, H. N. Tsao, C. Yi, A. K. Chandiran, M. K. Nazeeruddin, E. W.-G. Diau, C.-Y. Yeh, S. M. Zakeeruddin, M. Grätzel, *Science* **2011**, *334*, 629.
- [6] W. Zeng, Y. Cao, Y. Bai, Y. Wang, Y. Shi, M. Zhang, F. Wang, C. Pan, P. Wang, *Chem. Mater.* **2010**, *22*, 1915.
- [7] A. Listorti, B. O'Regan, J. R. Durrant, *Chem. Mater.* **2011**, *23*, 3381.
- [8] A. Hagfeldt, G. Boschloo, L. Sun, L. Kloo, H. Pettersson, *Chem. Rev.* **2010**, *110*, 6595.
- [9] a) M. Velusamy, K. R. Justin Thomas, J. T. Lin, Y.-C. Hsu, K.-C. Ho, *Org. Lett.* **2005**, *7*, 1899; b) K. R. Justin Thomas, J. T. Lin, Y.-C. Hsu, K.-C. Ho, *Chem. Commun.* **2005**, 4098; c) M.-S. Tsai, Y.-C. Hsu, J. T. Lin, H.-C. Chen, C.-P. Hsu, *J. Phys. Chem. C* **2007**, *111*, 18785; d) K. R. Justin Thomas, Y.-C. Hsu, J. T. Lin, K.-M. Lee, K.-C. Ho, C.-H. Lai, Y.-M. Cheng, P.-T. Chou, *Chem. Mater.* **2008**, *20*, 1830; e) Y.-S. Yen, Y.-C. Hsu, J. T. Lin, C.-W. Chang, C.-P. Hsu, D.-J. Yin, *J. Phys. Chem. C* **2008**, *112*, 12557; f) S.-T. Huang, Y.-C. Hsu, Y.-S. Yen, H.-H. Chou, J. T. Lin, C.-W. Chang, C.-P. Hsu, C. Tsai, D.-J. Yin, *J. Phys. Chem. C* **2008**, *112*, 19739; g) J. T. Lin, P.-C. Chen, Y.-S. Yen, Y.-C. Hsu, H.-H. Chou, M.-C. P. Yeh, *Org. Lett.* **2009**, *11*, 97; h) M. Velusamy, Y.-C. Hsu, J. T. Lin, C.-W. Chang, C.-P. Hsu, *Chem.*

- Asian J.* **2010**, *5*, 87; i) C.-H. Chen, Y.-C. Hsu, H.-H. Chou, K. R. Justin Thomas, J. T. Lin, C.-P. Hsu, *Chem. Eur. J.* **2010**, *16*, 3184.
- [10] a) Y.-J. Cheng, S.-H. Yang, C.-S. Hsu, *Chem. Rev.* **2009**, *109*, 5868; b) P.-L. T. Boudreault, A. Naraji, M. Leclerc, *Chem. Mater.* **2011**, *23*, 456.
- [11] D. W. Hawkins, B. Iddon, S. Darren, S. Longthorneb, P. J. Rosyk, *J. Chem. Soc. Perkin Trans. 1* **1994**, 2735.
- [12] J. K. Stille, *Angew. Chem.* **1986**, *98*, 504; *Angew. Chem. Int. Ed. Engl.* **1986**, *25*, 508.
- [13] a) A. K.-Y. Jen, V. P. Rao, K. Y. Wong, K. J. Drost, *J. Chem. Soc. Chem. Commun.* **1993**, 90; b) V. P. Rao, Y. M. Cai, A. K.-Y. Jen, *J. Chem. Soc. Chem. Commun.* **1994**, 1689; c) A. K.-Y. Jen, Y. Cai, P. V. Bedworth, S. R. Marder, *Adv. Mater.* **1997**, *9*, 132; d) S.-S. P. Chou, C.-H. Shen, *Tetrahedron Lett.* **1997**, *38*, 6407.
- [14] J. March, *Advanced Organic Chemistry*, 4th ed., Wiley, New York, **1992**, p. 45.
- [15] Y. J. Chang, T. J. Chow, *Tetrahedron* **2009**, *65*, 4726.
- [16] D. P. Hagberg, T. Marinado, K. M. Karlsson, K. Nonomura, P. Qin, G. Boschloo, T. Brinck, A. Hagfeldt, L. Sun, *J. Org. Chem.* **2007**, *72*, 9550.
- [17] a) K. R. Justin Thomas, J. T. Lin, Y.-Y. Lin, C.-T. Tsai, S.-S. Sun, *Organometallics* **2001**, *20*, 2262; b) Y.-J. Su, J. T. Lin, Y.-T. Tao, C.-W. Ko, S.-C. Lin, S.-S. Sun, *Chem. Mater.* **2002**, *14*, 1884; c) T.-H. Huang, J. T. Lin, L.-Y. Chen, Y.-T. Lin, C.-C. Wu, *Adv. Mater.* **2006**, *18*, 602.
- [18] Y.-S. Yen, Y.-C. Chen, Y. C. Hsu, H.-H. Chou, J. T. Lin, D.-J. Yin, *Chem. Eur. J.* **2011**, *17*, 6781.
- [19] Q-CHEM, Version 4.0, Y. Shao, L. Fusti-Molnar, Y. Jung, J. Kussmann, C. Ochsenfeld, S. T. Brown, A. T. B. Gilbert, L. V. Slipchenko, S. V. Levchenko, D. P. O'Neill, R. A. DiStasio, Jr., R. C. Lochan, T. Wang, G. J. O. Beran, N. A. Besley, J. M. Herbert, C. Y. Lin, T. Van Voorhis, S. H. Chien, A. Sodt, R. P. Steele, V. A. Rassolov, P. E. Maslen, P. P. Korambath, R. D. Adamson, B. Austin, J. Baker, E. F. C. Byrd, H. Dachsel, R. J. Doerksen, A. Dreuw, B. D. Dunietz, A. D. Dutoi, T. R. Furlani, S. R. Gwaltney, A. Heyden, S. Hirata, C.-P. Hsu, G. Kedziora, R. Z. Khaliullin, P. Klunzinger, A. M. Lee, M. S. Lee, W. Liang, I. Lotan, N. Nair, B. Peters, E. I. Proynov, P. A. Pieniazek, Y. M. Rhee, J. Ritchie, E. Rosta, C. D. Sherrill, A. C. Simmonett, J. E. Subotnik, H. L. Woodcock III, W. Zhang, A. T. Bell, A. K. Chakraborty, D. M. Chipman, F. J. Keil, A. Warshel, W. J. Hehre, Z. Gan, Y. Zhao, N. E. Schultz, D. Truhlar, E. Epifanovsky, M. Oana, R. Baer, B. R. Brooks, D. Casanova, J.-D. Chai, C.-L. Cheng, C. Cramer, D. Crittenden, A. Ghysels, G. Hawkins, E. G. Hohenstein, C. Kelley, W. Kurlancheck, D. Liotard, E. Livshits, P. Manohar, A. Marenich, D. Neuhauser, R. Olson, M. A. Rohrdanz, K. S. Thanthiriwatte, A. J. W. Thom, V. Vanovschi, C. F. Williams, Q. Wu, Z.-Q. You, Sundstrom, E.; Parkhill, J.; Lawler, K.; Lambrecht, D.; Goldey, M.; Olivares-Amaya, R.; Bernard, Y.; Vogt, L.; Watson, M.; Liu, J.; Yeganeh, S.; Kaduk, B.; Vydrov, O.; Xu, X.; Zhang, C.; Russ, N.; Zhang, I. Y.; Goddard III, W. A.; Besley, N.; Ghysels, A.; Landau, A.; Wormit, M.; Dreuw, A.; Diedenhofen, M.; Klamt, A.; Lange, A. W.; Ghosh, D.; Kosenkov, D.; Landou, A.; Zuev, D.; Deng, J.; Mao, S. P.; Su, Y. C.; Small D.; H. F. Schaefer III, J. Kong, A. I. Krylov, P. M. W. Gill, and M. Head-Gordon, Q-Chem, Inc., Pittsburgh, PA, **2008**.
- [20] a) H. M. Vaswani, C.-P. Hsu, M. Head-Gordon, G. R. Fleming, *J. Phys. Chem. B* **2003**, *107*, 7940; b) Y. Kurashige, T. Nakajima, S. Kurashige, K. Hirao, Y. Nishikitani, *J. Phys. Chem. A* **2007**, *111*, 5544.
- [21] a) N. Hirata, J.-J. Lagref, E. J. Palomares, J. R. Durrant, M. K. Nazeeruddin, M. Grätzel, D. Di Censo, *Chem. Eur. J.* **2004**, *10*, 595; b) J. R. Durrant, S. A. Haque, E. Palomares, *Chem. Commun.* **2006**, 3279; c) A. Dreuw, M. Head-Gordon, *J. Am. Chem. Soc.* **2004**, *126*, 4007.

Received: January 2, 2012
Published online: March 15, 2012